

# Design and Performance Analysis of a 1550nm $\text{Al}_{0.09}\text{Ga}_{0.38}\text{In}_{0.53}\text{As}/\text{InP}$ MQW VCSEL by Varying Injection Current

Tamal Roy, Avijit Das, Sujan Howlader, Md. Ronok Hasan Rubel and Rinku Basak

**Abstract**– The Vertical-Cavity Surface-Emitting Laser (VCSEL) is becoming a key device in high-speed optical local-area networks (LANs) and even wide-area networks (WANs). This device is also enabling ultra parallel data transfer in equipment and computer systems. In this work, the performance characteristics of a designed AlGaInAs/InP based 1550nm multiple quantum well (MQW) VCSEL have been obtained through computations. The obtained characteristics have been analyzed for obtaining better performance. For achieving a superior performance, the concentrations of AlGaInAs QW material have been chosen using the results of other research works. The material gain of a compressive strained  $\text{Al}_{0.09}\text{Ga}_{0.38}\text{In}_{0.53}\text{As}/\text{InP}$  MQW VCSEL has been theoretically computed. Using the peak material gain obtained from this computation the performance characteristics of the designed VCSEL have been obtained. At 300K, the threshold current of the VCSEL has been obtained as 0.61mA. A maximum output power of 2.24mW has been obtained for this designed VCSEL at 6.1mA injection current. Corresponding to the frequency modulation, the maximum resonance frequency has been obtained as 7.7GHz at 6.1mA injection current which indicates high speed performance of the designed VCSEL. By varying injection current the characteristics of designed VCSEL have also been obtained.

**Keywords**– Laser Diode, VCSEL and MQW

## I. INTRODUCTION

The Vertical Cavity Surface Emitting Laser (VCSEL) is a technology that has come to great importance in the optical communications field. From the time that researchers first developed the VCSEL to now with many different abilities and realizations of VCSEL available

**Tamal Roy** is a Graduate of American International University-Bangladesh (AIUB), Banani, Dhaka-1213, Bangladesh. Email: tamalroy724@gmail.com

**Avijit Das** is a Graduate of American International University-Bangladesh (AIUB), Banani, Dhaka-1213, Bangladesh. Email: savijits@gmail.com

**Sujan Howlader** is a Graduate student of American International University-Bangladesh (AIUB), Banani, Dhaka-1213, Bangladesh. Email: essan99@gmail.com

**Md. Ronok Hasan Rubel** is an Undergraduate student of American International University-Bangladesh (AIUB), Banani, Dhaka-1213, Bangladesh. Email: rhtdm.np@gmail.com

**Rinku Basak** is an Assistant Professor and Head (Graduate Program), Department of EEE, Faculty of Engineering, American International University-Bangladesh (AIUB), Banani, Dhaka-1213, Bangladesh. Email: rinku\_biju@yahoo.com, rinku@aiub.edu

commercially today, VCSEL has made its use in many different current-technology applications [1]. The importance of vertical-cavity surface-emitting lasers (VCSELs) to the telecommunications industry is growing rapidly. VCSELs are more cost-efficient to mass-produce, and have better fiber coupling efficiencies than the edge-emitting semiconducting lasers that are the current industry standard. Also, VCSELs in a single longitudinal mode, and thus are not prone to mode hopping, and have a circularly symmetric output beam that can be tightly focused. Currently, VCSELs power most short-distance (under 300meter) optical links because they operate in the 850nm transmission window. However, there has been recent progress in the development of VCSELs that operate at the 1310 nm or 1550 nm transmission windows required for long-distance communications [2].

Long-wavelength vertical-cavity surface-emitting lasers (LW-VCSELs) are attractive light sources because of their unique features such as low power consumption, narrow beam divergence, and ease of fabricating two-dimensional array. Although power consumption of optical transceivers in long-wavelength fiber-optic communication systems has been reduced, that of semiconductor lasers used as light sources for optical transceivers still remains high. It is expected that further power consumption reduction for optical transceivers can be achieved by using LW-VCSELs [3].

LW-VCSELs are categorized into two types according to their substrates: One is GaAs-based VCSELs with GaInNAs active layers and the other is InP-based VCSELs with AlGaInAs or GaInAsP active layers. InP-based LW-VCSELs use buried tunnel junction (BTJ) for current confinement, thereby greatly improving performance. In GaAs-based LW-VCSELs, AlGaAs oxide current confinement structure is widely used due to the advantage of using epitaxial growth technique for those compound materials. AlGaInAs/InP VCSELs have been mostly designed for wavelength of 1550nm and above which are mostly suitable for long telecommunication [3].

It is well known that the small active volume and high mirror reflectivity of a VCSEL contribute to its very low threshold current. With this low threshold current VCSELs allow high-speed operation around 10Gbps in data transmission over the optical fiber.

In this work, the performance characteristics of a designed 1550nm AlGaInAs/InP MQW VCSEL have been obtained considering injection current effect. The obtained characteristics have been analyzed and presented in this work with the aim of the better performance of the VCSEL.

**II. DESIGN OF A AlGaInAs/InP 1550nm MQW VCSEL STRUCTURE**

**A. Design of the Active region and the cavity of the VCSEL**

In this work, a VCSEL whose active region contains three QWs of  $Al_{0.09}Ga_{0.38}In_{0.53}As$  separated by InP barriers is chosen for simulation with a view to obtaining 1550nm operation. Fig.1 shows the cavity of the VCSEL consists two cladding layers of  $Al_{0.6}Ga_{0.4}As$ .The cladding and active layer materials are separated by two separate confinement heterostructure(SCH) layers of InP. On the top and bottom of 3QW cavity active region upper and lower Distributed Bragg Reflector (DBR) stacks are formed. The lattice constant of QW and barrier material is  $5.869\text{\AA}$ .

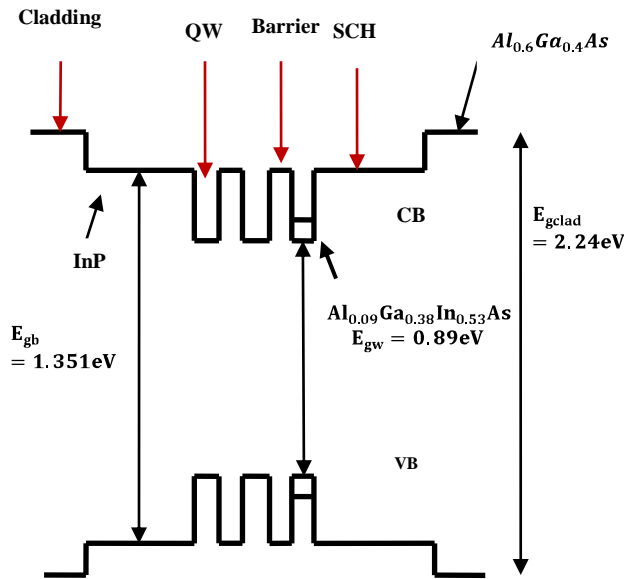


Fig. 1: The active region of a VCSEL consisting 3 quantum wells of  $125\text{\AA}$  each

The temperature dependence of energy gap in AlGaInAs has been modeled with the Varshni equation as [4],

$$E_g(T) = E_g(T=0K) - \frac{\alpha T^2}{\beta + T} \quad (1)$$

where,  $\alpha$  and  $\beta$  are the experimental fitting parameters.

After computations, InP based quaternary compound semiconductor material  $Al_{0.09}Ga_{0.38}In_{0.53}As$  has been chosen quantum well material whose band gap energy is calculated of  $0.89\text{eV}$ . The  $E_g$  of barrier material, InP is calculated as  $1.351\text{eV}$  and the  $E_g$  of cladding material,  $Al_{0.6}Ga_{0.4}As$  is calculated as  $2.24\text{eV}$ . Values of a number of parameters are obtained from different published sources [5], [6].

The structure of the VCSEL is presented in Fig. 2. The thickness of each QW is chosen to be  $125\text{\AA}$  and each barrier is chosen to be  $170\text{\AA}$ . The active region of the VCSEL is separated by two upper and lower DBR stacks. The VCSEL consists of 8 layer of Si/SiO<sub>2</sub> material in the upper DBR stacks(p-type) and 77 layers of  $Al_{0.15}Ga_{0.32}In_{0.53}As/InP$

materials in the bottom DBR stack(n-type) which is placed on n-type InP substrate as shown in Fig. 2. The current is injected through the upper p-type contact and the lower n-type contact is connected with the substrate.

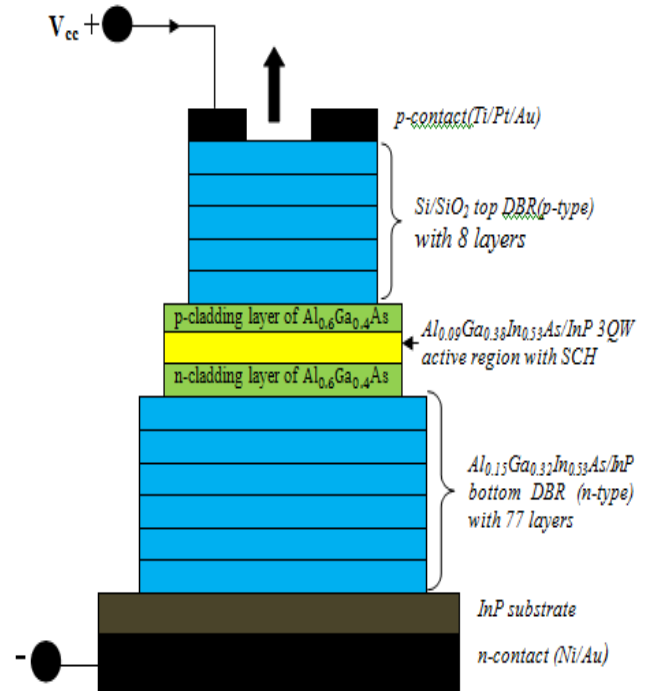


Fig. 2: The designed structure of a top-emitting 1550nm  $Al_{0.15}Ga_{0.32}In_{0.53}As/InP$  MQW VCSEL

**B. Calculation of Material gain**

For designing a VCSEL structure the material gain is calculated as [7-12],

$$g(E) = \left( \frac{q^2 \pi \hbar}{\epsilon_0 m_0^2 n c E} \right) |M_T|^2 \rho_r (f_2 - f_1) \quad (2)$$

where,  $q$  is the electron charge,  $\epsilon_0$  is the free-space permittivity,  $c$  is the vacuum speed of light,  $n$  is the refractive index of the laser structure,  $E$  is the transition energy,  $m_0$  is the mass of electron.  $|M_T|^2$  is the transition momentum matrix element.  $\rho_r$  is the reduced density of state.  $\hbar$  is the Plank's constant divided by  $2\pi$ ,  $f_2$  and  $f_1$  are the electron quasi Fermi functions in the conduction and valance band respectively.

It is important to compute the material gain using equation (2) and to obtain the plot of material gain vs. photon density and material gain vs. wavelength. It is important to arrange so that the cavity oscillation occurs at the peak value of the gain of the material. The reduced density of state  $\rho_r$ , is calculated as  $1.0263 \times 10^{44}$ . The split off band potential  $\Delta$  has been found to be  $0.361\text{eV}$ .The square of the transition momentum matrix ( $|M_T|^2$ ) of a laser with quantum well region is calculated as  $3.9481 \times 10^{-30}$ . After plotting the obtained results the plots are presented in Fig. 3 and Fig. 4.

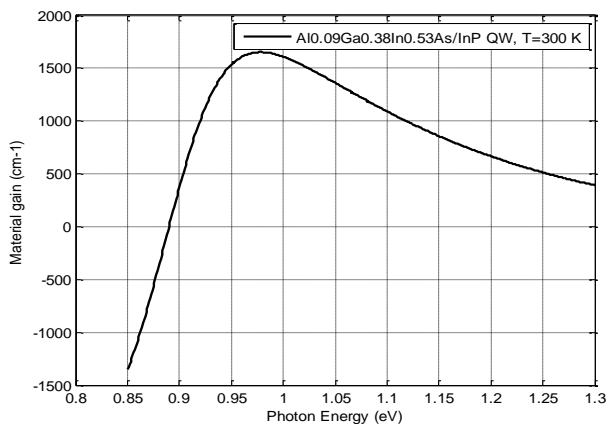


Fig. 3: Plot of material gain for  $\text{Al}_{0.09}\text{Ga}_{0.38}\text{In}_{0.53}\text{As}/\text{InP}$  125Å QW by varying photon energy at 300K. A maximum gain of the material of  $1652.3\text{cm}^{-1}$  is obtained

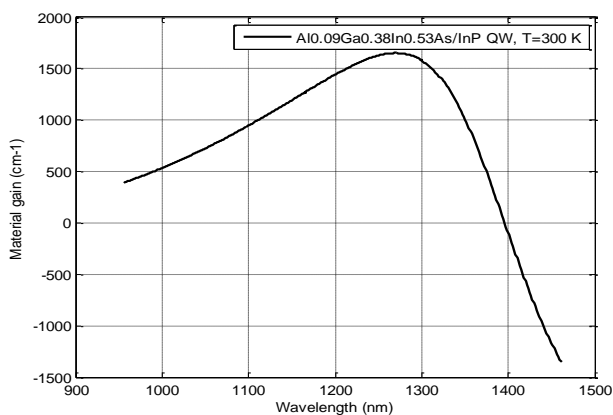


Fig. 4: Plot of material gain for  $\text{Al}_{0.09}\text{Ga}_{0.38}\text{In}_{0.53}\text{As}/\text{InP}$  125Å MQW by varying wavelength at 300K. A maximum gain of the material of  $1652.3\text{cm}^{-1}$  is obtained.

It is observed that at 0.89eV the material gain goes to positive level and a maximum gain is obtained as  $1652.3\text{cm}^{-1}$  at 1270.3nm wavelength. It is observed that the peak gain of the materials in the QW shifts to lower wavelength value from 1550nm.

### C. Cavity length and cavity volume

For this VCSEL the optical cavity length is along the direction of the flow of photons and carriers which is the vertical direction. Various research papers indicate that the optical cavity of a VCSEL should be between one and a half wavelengths to three wave lengths at the lasing wavelength. For this VCSEL the designed cavity length is taken as  $1.5\lambda$  i.e,  $1.5 \times 1550 = 2325\text{nm}$ .

The values of the effective contribution from the top and bottom DBRs need to be added with this value to obtain the  $L_{\text{eff}}$  as shown below  $L_{\text{eff}} = L_{\text{cavity}} + L_{\text{eff-Top}} + L_{\text{eff-bottom}} = 1904\text{nm}$ .

The effective length of the top and bottom Bragg reflector may be written as  $L_{\text{eff}} = \lambda/4\Delta n$ , where,  $\Delta n$  is the refractive index difference between top and bottom DBR stacks. The active volume of designed VCSEL is  $3.7575 \times 10^{-12}\text{cm}^3$ .

### D. Confinement factor, transparency carrier density and threshold carrier density of the laser

The optical confinement factor  $\Gamma$ , with an enhancement factor of 2, assuming 90% confinement in the transverse direction is 0.0355 computed using the equation described in [7]. The analytical expression for computing the transparency carrier density is [7],

$$N_{\text{tr}} = 2 \left( \frac{kT}{2\pi\hbar^2} \right)^{3/2} (m_c m_v)^{3/4} \quad (3)$$

where,  $k$  is the Boltzmann const,  $T$  is the temperature in K,  $\hbar$  is the Plank's constant divided by  $2\pi$ ,  $m_c$  and  $m_v$  are the effective masses of carriers in the CB and VB respectively. This relation is used to compute the transparency carrier density of QW and barrier materials.

At 300K the calculated value of the transparency carrier densities of InP is obtained as  $2.5301 \times 10^{18}\text{cm}^{-3}$  and the same for  $\text{Al}_{0.09}\text{Ga}_{0.38}\text{In}_{0.53}\text{As}$  as  $1.3780 \times 10^{18}\text{cm}^{-3}$ . For lower transparency carrier density of  $\text{Al}_{0.09}\text{Ga}_{0.38}\text{In}_{0.53}\text{As}$  compared to InP makes it is suitable to use it as a QW material and InP is chosen as a barrier material. The carrier density at threshold ( $N_{\text{th}}$ ) is calculated as  $2.1208 \times 10^{18}\text{cm}^{-3}$ .

### E. Differential quantum efficiency and Power of the VCSEL

The differential quantum efficiency of the designed  $\text{Al}_{0.09}\text{Ga}_{0.38}\text{In}_{0.53}\text{As}/\text{InP}$  MQW VCSEL is also calculated in this work. The differential quantum efficiency of VCSELs is expressed as [10],

$$\eta_d = \eta_i \frac{\alpha_m}{\{<\alpha_i> + \alpha_m\}} \quad (4)$$

where,  $\eta_i$  is the current injection efficiency,  $\alpha_i$  is the intrinsic absorption loss coefficient,  $\alpha_m$  is the mirror loss of a VCSEL.

By considering  $20\text{cm}^{-1}$  internal loss due to absorption in the material of the cavity the calculated value of differential quantum efficiency of the designed  $\text{Al}_{0.09}\text{Ga}_{0.38}\text{In}_{0.53}\text{As}/\text{InP}$  MQW VCSEL is obtained as 16.65%. A suitable efficiency improves the performance of the designed VCSEL and makes the VCSEL suitable for performing in high speed communications.

The output power ( $P_o$ ) of the VCSEL can be expressed as [7], [13], [14],

$$P_o = \frac{\alpha_m h v \eta_i}{q g \Gamma} (I - I_{\text{th}}) \quad (5)$$

where,  $P_o$  is the output power,  $\alpha_m$  is the mirror loss coefficient,  $h$  is the Plank's constant,  $v$  is the lasing frequency,  $q$  is the electron charge,  $g$  is the material gain,  $\Gamma$  is the confinement factor,  $\eta_i$  is the injection efficiency,  $I$  is the injection current and  $I_{\text{th}}$  is the threshold current of the device.

The output power of 2.24mW has been obtained for this designed VCSEL at 6.1mA injection current.

**F. Computation of photon life time  $\tau_p$  of the VCSEL**

For calculating the photon lifetime, if the intrinsic absorption loss is taken as  $\alpha_i = 20 \text{ cm}^{-1}$ , photon lifetime  $\tau_p$  may be computed as  $4.3932 \times 10^{-12}$  sec using equation in [7],

$$\tau_p = \frac{1}{(\nu_g \times (\alpha_i + \alpha_m))} \tag{6}$$

**G. Computation of threshold current  $I_{th}$  of the VCSEL**

The equation for the threshold current is given as [10], [13], [14]:

$$I_{th} = \frac{qV_a N_{th}}{\eta_i \tau_c} \tag{7}$$

For a current injection efficiency ( $\eta_i$ ) of 0.8 and the carrier lifetime ( $\tau_c$ ) =  $2.63 \times 10^{-9}$  sec, the threshold current is found to be 0.61 mA.

**H. Solution of rate equations**

For finite order differential solution of the rate equation, the following table of parameters has been used. Some of the values have been taken from reference and carried forward from table and previous calculation.

Table 1: List of parameters to be used to find out the solution to rate equations

Parameter Type	Value
Length of the active region, $L_a$	$3.75 \times 10^{-6}$ cm
Effective length of the cavity region, $L_{eff}$	$190.4 \times 10^{-6}$ cm
Average refractive index, $n$	3.264
Current injection efficiency( $\eta_i$ )	0.8
Carrier lifetime ( $\tau_c$ )	$2.63 \times 10^{-9}$ sec
Peak material Gain coefficient ( $g_0$ )	1652.3cm-1
Differential gain (a)	$10 \times 10^{-16}$ cm <sup>2</sup>
Stationary electronic mass ( $m_0$ )	$9.1 \times 10^{-31}$ kg
Intrinsic absorption loss ( $\alpha_i$ )	20 cm <sup>-1</sup>
Reflectivity(R) of both the mirrors	0.999
Gain compression factor( $\epsilon$ )	$1.5 \times 10^{-17}$
Spontaneous emission factor ( $\beta_{sp}$ )	$1.69 \times 10^{-4}$
Transparency carrier density( $N_{tr}$ )	$1.378 \times 10^{18}$ cm <sup>-3</sup>
Carrier density at threshold point( $N_{th}$ )	$2.1208 \times 10^{18}$ cm <sup>-3</sup>
The threshold current( $I_{th}$ )	0.61 mA
Photon lifetime ( $\tau_p$ )	$4.3932 \times 10^{-12}$ sec

Now all of the required parameters have been gathered for solving the rate equations [10],

The rate of change of carrier density of a laser is written as [10],

$$\frac{dN}{dt} = \eta_i \frac{I}{qV_a} - \frac{N}{\tau_c} - \frac{\nu_g a (N - N_{tr})S}{(1 + \epsilon S)} \tag{8}$$

The rate of change of photon density of a Laser is written as [10]:

$$\frac{dS}{dt} = \frac{\Gamma \nu_g a (N - N_{tr})S}{1 + \epsilon S} + \Gamma \beta_{sp} \frac{\eta_i I_{th}}{q} - \frac{S}{\tau_p} \tag{9}$$

where, N is the carrier density, S is the photon density, I is the injection current, q is the electron charge,  $V_a$  is the volume of the active region,  $\eta_i$  is the injection efficiency,  $\tau_c$  is the carrier life time,  $\nu_g$  is the group velocity, a is the differential gain,  $N_{tr}$  is the transparency carrier density,  $\epsilon$  is the gain saturation parameter,  $\beta_{sp}$  is the spontaneous emission coefficient,  $\Gamma$  is the coefficient factor,  $\tau_c$  is the photon lifetime and  $I_{th}$  is the threshold current of a laser.

This solution of the differential equations is obtained by finite difference method. The two important coupled rate equations: (i) the rate equation for carrier density and (ii) the rate equation for photon density are solved simultaneously for a chosen value of injection current (6.1mA). The value of the injection current is to be taken above the threshold current. The solution has been performed using MATLAB.

Using the output of this computation work a plot of carrier density versus time is obtained for the designed 1550nm VCSEL. This plot is presented in fig 5. It is observed from this plot that following the current injection, the carrier density value increases almost linearly at the beginning and shows an overshoot up to  $4.32 \times 10^{18}$  cm<sup>-3</sup>. This value stabilizes to steady value of  $2.831 \times 10^{18}$  cm<sup>-3</sup> after about 2ns from the beginning as is observed from Fig. 5.

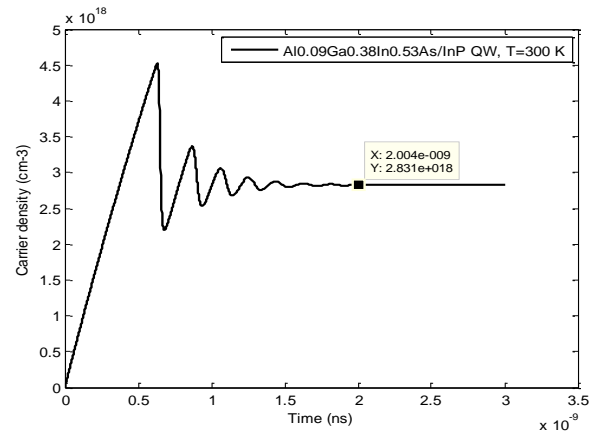


Fig. 5: Plot of carrier density vs. time of a 1550nm Al<sub>0.09</sub>Ga<sub>0.38</sub>In<sub>0.53</sub>As/InP 125Å QW VCSEL at 300K, where, the injection current is 6.1mA

Using the output of the same computation work mentioned above, a plot of photon density versus time is obtained for the designed 1550nm VCSEL. This plot is presented in Fig. 6. It is observed from this plot that, similar to the carrier density plot, following the current injection, the photon density value increases almost linearly at the beginning and shows an overshoot up to  $1.766 \times 10^{16}$  cm<sup>-3</sup>. This value stabilizes after 5 to 8 oscillatory swing to a steady value of  $1.09941 \times 10^{15}$  cm<sup>-3</sup> after about 2.286ns from the beginning as is observed from Fig. 6.



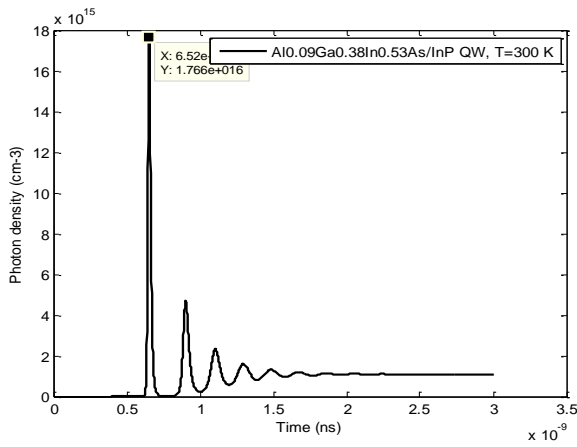


Fig. 6: Plot of photon density vs. time of a 1550nm Al<sub>0.09</sub>Ga<sub>0.38</sub>In<sub>0.53</sub>As/InP 125Å QW VCSEL at 300K, where, the injection current is 6.1mA

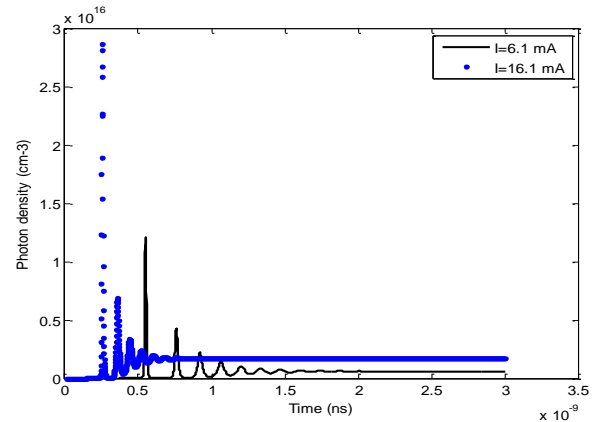


Fig. 8: Plots of photon density vs. time for different values of injection current of a Al<sub>0.09</sub>Ga<sub>0.38</sub>In<sub>0.53</sub>As/InP 125Å QW VCSEL at 300K

### III. PERFORMANCE CHARACTERISTICS OF THE DESIGNED VCSEL

The variations of injection current for obtaining performance analysis are as follows:

This section is dedicated entirely to the find the variation in the characteristics of the designed VCSEL with variation of injection current. The injection current is varied from a value of 6.1 mA to 16.1 mA with an interval of 10 mA. MATLAB simulation tool is used for determining the characteristics of the laser under these conditions. The plots of carrier density vs. time and photon density vs. time are obtained with the variation of injection current shown in Fig. 7 and Fig. 8.

It is observed that the carrier density and photon density increases with the value of injection current, where the threshold current of the device is 0.61mA.

The relationship between material gain and photon density indicates that positive gain makes a VCSEL suitable for high photon output which enhances the output power of the laser. A high output power contributes to the high modulation bandwidth which enhances the dynamic performance of the VCSEL. The transfer function of relative response of a VCSEL is related to the resonance frequency  $f_R$  and damping parameter  $\gamma$ ; and the well known expression is written as [10], [13], [14]:

$$H(f) = \frac{f_R^2}{f_R^2 - f^2 + j \frac{f}{2\pi} \gamma} \quad (10)$$

Using equation (10), the relative response of the VCSEL has been calculated by varying frequency for different values of injection current. The obtained results are plotted as shown in fig 9. It is observed that with increase of injection current the resonance frequency as well as the modulation bandwidth of the VCSEL increases. And higher modulation bandwidth makes the VCSEL suitable for transmitting data at high speed through optical fiber.

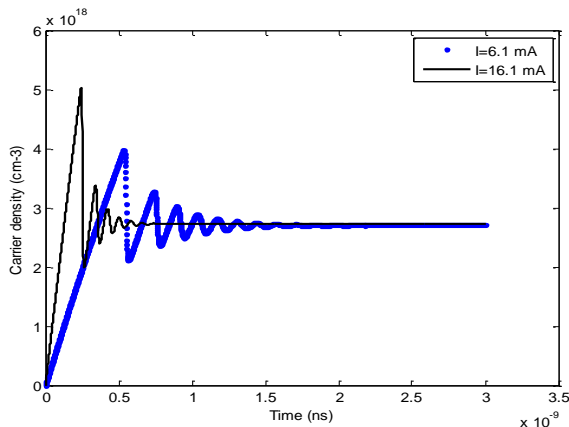


Fig. 7: Plots of carrier density vs. time for different values of injection current of a Al<sub>0.09</sub>Ga<sub>0.38</sub>In<sub>0.53</sub>As/InP 125Å QW VCSEL at 300K

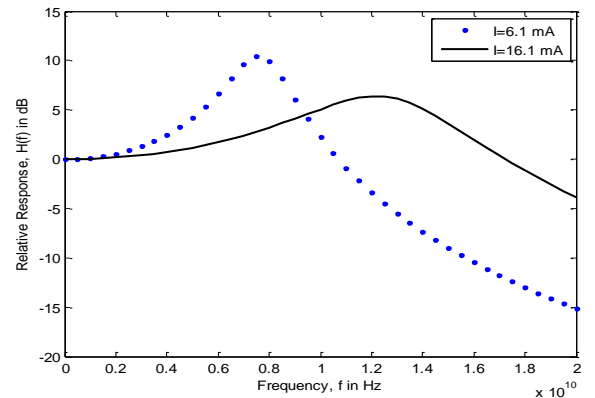


Fig. 9: Plots of relative response vs. frequency for different value of injection current of a Al<sub>0.09</sub>Ga<sub>0.38</sub>In<sub>0.53</sub>As/InP 125Å QW VCSEL at 300K

The resonance frequency of the VCSEL increases from 7.7GHz to 12.3GHz by increasing the injection current from 6.1mA to 16.1mA and maximum modulation bandwidth is obtained as 19.3GHz.

### IV. CONCLUSION

In this work, a 1550nm VCSEL has been designed theoretically using MQWs with the quaternary compound Al<sub>0.09</sub>Ga<sub>0.38</sub>In<sub>0.53</sub>As as the well material and the binary compound InP as the barrier material, Si/SiO<sub>2</sub> top DBR system and Al<sub>0.15</sub>Ga<sub>0.32</sub>In<sub>0.53</sub>As/InP bottom DBR system with Ti/Pt/Au as the p-side contact and Ni/Ge/Au as the n-side

contact. In the active region, three quantum wells and two barrier materials have been used. Two SCH layers of InP (same as the barrier), a p-cladding layer made of  $\text{Al}_{0.6}\text{Ga}_{0.4}\text{As}$  (doped with Si) and an n-cladding layer made of  $\text{Al}_{0.6}\text{Ga}_{0.4}\text{As}$  (doped with Be) have used. The optical cavity length has been adjusted to 1.5 wavelengths. The materials of all the layers are almost lattice matched throughout the entire structure of the VCSEL which makes it suitable for fabrication using epitaxial growth technology. Computations show that, at 300K the threshold current of the VCSEL is obtained as 0.61mA. A maximum output power of 2.24mW is obtained at 6.1mA injection current and for the same value of injection current a maximum resonance frequency is obtained as 7.7GHz. The transparency carrier density at this temperature is  $1.378 \times 10^{18} \text{ cm}^{-3}$ . The threshold carrier density at this temperature of 300K is  $2.1208 \times 10^{18} \text{ cm}^{-3}$ , the steady state carrier density  $2.831 \times 10^{18} \text{ cm}^{-3}$  and steady state photon density of  $1.09941 \times 10^{15} \text{ cm}^{-3}$ . The enhanced performance of the VCSEL is obtained by increasing the injection current from 6.1mA to 16.1mA. A maximum resonance frequency of 12.3GHz and the corresponding modulation bandwidth is obtained as 19.3GHz at 16.1mA injection current which enhance the high speed performance of the device.

The performance characteristics curves show acceptable performance. The VCSEL is expected to perform well after fabrication.

## REFERENCES

- [1] Kenichi Iga, Fellow, IEEE, "Surface-Emitting Laser—Its Birth and Generation of New Optoelectronics Field", IEEE Journal on selected topics in Quantum Electronics, Vol. 6, No. 6, November/December 2000.
- [2] David F. Welch, Senior Member, IEEE, "A Brief History of High-Power Semiconductor Lasers", IEEE Journal on selected topics in Quantum Electronics, VOL. 6, NO. 6, NOVEMBER/DECEMBER 2000
- [3] Yut aka ONISHI\*, Nobuhiro SAGA, Kenji KOYAMA, Hideyuki DOI, Takashi ISHIZUKA, Takashi YAMADA, Kosuke FUJII, Hiroki MORI, Jun-ichi HASHIMOTO, Mitsuru SIMAZU, Akira YAMAGUCHI and Tsukuru KATSUYAMA," Long-wavelength GaInNAs VCSEL With Buried Tunnel Junction Current Confinement Structure", SEI TECHNICAL REVIEW NUMBER 68 · APRIL 2009.
- [4] Z. Pan, L.H. Li, Y. W. Lin, B. Q. Sun, D. S. Jiang and W. K. Ge, "Conduction band offset and electron effective mass in GaInNAs/GaAs quantum-well structures with low nitrogen concentration", Applied Physics Letters, Vol. 78, No.15,2001,pp.2217-1-2217-3.
- [5] I. Vurgaftman, J. R. Meyer R. Ram-Mohan, "Band parameters for III-V compound semiconductors and their alloys" , JOURNAL OF APPLIED PHYSICS , Vol. 89, No. 11, 1 June 2001 Appl. Phys. Rev.: Vurgaftman, Meyer, and Ram-Mohan, pp.5815-5875.
- [6] S. Adachi, "Properties of Semiconductor Alloys Group-IV, III-V, II-VI Semiconductor", John Wiley & Sons, New York, 2009, pp.133-214,238-253,277-286,307-332.
- [7] T. E. Sale, Vertical Cavity Surface Emitting Lasers, John Wiley, 2005, pp.1-106.
- [8] P. Harrison, Quantum wells, Wires and Dots, 2<sup>nd</sup> edition, John Wiley, England, 2005, pp.1-71.
- [9] S. L. Chuang, Physics of Optoelectronics Devices, John Wiley, New York, 1995, pp.394-483.
- [10] L. A. Coldren, S. W. Corzine, Diode Lasers and Photonic Integrated Circuits, Wiley, New York, 1995, pp.1-261.
- [11] Y. A. Chang, J. R. Chen, H. C. Kuo, Y. K. Kuo, and S.C. Wang, "Theoretical and Experimental Analysis on InAlGaAs/AlGaAs Active Region of 850nm VCSELs", Journal of Lightwave Technology, vol.24, No. 1, January 2006, pp.536-543.
- [12] T. A. Ma, Z. M. Li, T. Makino, and M. S. Wartak, "Approximate Optical Gain Formulas for 1.55- $\mu\text{m}$  Strained Quantum-Well Lasers", IEEE Journal of Quantum Electronics, vol. 31, No. 1, May 1995, pp.29-34.
- [13] Rinku Basak and Saiful Islam, "Performance Analysis of a 980nm  $\text{In}_{0.2}\text{Ga}_{0.8}\text{As}/\text{GaAs}$  MQW VCSEL Considering Thermal Effect", The AIUB Journal of Science and Engineering (AJSE), Volume 10 No.1 August 2011.
- [14] Rinku Basak and Saiful Islam, "Optimization of a Near-Infrared 980nm VCSEL for obtaining Improved Modulation Performance", The AIUB Journal of Science and Engineering (AJSE)", Volume 11 No.1 August 2012.